Journal of Photochemistry and Photobiology A: Chemistry 222 (2011) 64–69

Contents lists available at ScienceDirect

Journal of Photochemistry and Photobiology A: Chemistry

journal homepage: www.elsevier.com/locate/jphotochem

# Wettability conversion and surface friction force variation of polycrystalline rutile ceramics under UV illumination

Kenji Okudaira[a], Tomoya Kato[b], Toshihiro Isobe[a], Sachiko Matsushita[a], Toshihiro Kogure[b], Akira Nakajima[a,*]

[a] Department of Metallurgy and Ceramics Science, Graduate School of Science and Engineering, Tokyo Institute of Technology, 2-12-1 O-okayama, Meguro-ku, Tokyo 152-8552, Japan
[b] Department of Earth and Planetary Sciences, Graduate School of Science, The University of Tokyo, 7-3-1 Hongo, Bunkyo-ku, Tokyo 113-0033, Japan

ARTICLE INFO

*Article history:*
Received 25 March 2011
Accepted 9 May 2011
Available online 17 May 2011

*Keywords:*
Titanium dioxide
Rutile
Friction
Friction force microscopy
Hydrophilicity

ABSTRACT

Photoinduced surface friction variations of the polished surface of polycrystalline rutile ceramics under UV illumination in different atmospheres was evaluated using FFM. When UV was irradiated onto the rutile surface, the surface friction force first increased and then decreased. Once the water contact angle of the rutile surface reached the lower limit, the surface friction force increased gradually. Increased friction force on the surface in the early stage of UV illumination was attributable to decomposition of the surface organic contaminant and the resultant increase of surface energy from the fitting of calculated contact angles to practical values. However, the friction force decrease and gradual increase after a certain period of UV illumination are attributed to the lubrication effect and either a capillary effect or the increased adsorbed water layer by humidity control. From the force curve measurement on the highly hydrophilic rutile single crystal (1 0 0), the repulsion force was detected from 2 to 3 nm separation distance.



## 1. Introduction

Since the discovery that $TiO_2$ can break down water, the photoinduced reaction of titanium dioxide [1] has been well studied, especially the strong oxidation power of photogenerated radical species [2] for water and air purification applications [3–6]. In addition to these conventional applications, the photoinduced hydrophilicity of a $TiO_2$ photocatalyst was discovered in 1995 [7]. A highly hydrophilic surface is generated when UV is irradiated onto the surface of $TiO_2$. This surface exhibits both antifogging and self-cleaning properties. Polycrystalline $TiO_2$ film coatings have been applied to various industrial items [8]. To date, two mechanisms have been proposed for this intriguing property: photocatalytic decomposition of surface organic contaminants [9,10] and photoinduced surface structural change [11,12].

These unique photochemical properties reflect differences in friction force. Several scientists have reported photoinduced friction force variation on a $TiO_2$ surface using friction force microscopy (FFM). Wang et al. revealed unique hydrophilic–hydrophobic domain structures on the rutile surface, which have oxygen bridging sites and which exhibit a high hydrophilic conversion rate [7,13]. Although detailed mechanisms of the generation of this specific structure remain unclear, these microdomains are regarded as acting as flow channels for water and oil, analogously to a two-dimensional capillary, thereby creating a highly hydrophilic surface. The appearance of a similar microstructure was confirmed also in anatase polycrystalline thin films during UV illumination [14]. For anatase polycrystalline thin films, it is deduced that the crystal face dependence of photoinduced hydrophilicizing rate provides the domain structures and the resultant highly hydrophilic state [15]. Recently, we investigated the dependence of the photoinduced friction force variation for anatase polycrystalline thin films by a plasma crystallization process on the UV intensity and atmosphere [16]. In this case, the photoinduced friction force variation for UV illumination time was divisible into two stages: decreasing and increasing. The decreasing stage was attributable to the photocatalytic decomposition of organic compound and the increase of hydrophilicity, whereas the increasing stage was attributed to the capillary effect or an increase in the adsorbed water layer.

However, residual stress from substrates reportedly affects photocatalytic activities of anatase thin films [17,18]. Moreover, detailed analyses of friction force change for each grain surface is infeasible for anatase because of its extremely fine grains. Therefore, comprehensive investigation of the relation between photoinduced wettability conversion and photoinduced friction force variation on the polycrystalline materials from each grain level has yet to be conducted.

For this study, we used rutile polycrystalline ceramics to avoid the influence from the substrate. Then we evaluated the friction

* Corresponding author. Tel.: +81 3 5734 2525; fax: +81 3 5734 3355.
*E-mail address:* anakajim@ceram.titech.ac.jp (A. Nakajima).

1010-6030/$ – see front matter © 2011 Elsevier B.V. All rights reserved.
doi:10.1016/j.jphotochem.2011.05.002

force of each grain directly under UV illumination in various atmospheres using FFM. The relation between the photoinduced friction force variation of rutile ceramic and its photoinduced hydrophilicity are discussed in detail. Moreover, force curve measurements using an atomic force microscope (AFM) was conducted under UV illumination for rutile single crystal to evaluate the attraction and repulsion interactions in ambient air.

## 2. Experimental

### 2.1. Sample preparation and characterization

For evaluation of the friction force of rutile grains in the observable range (10 μm × 10 μm) of FFM, we must prepare dense (relative density >98%) rutile ceramics with grain size of 2–3 μm. We performed preliminary experiments for sample preparation by changing the heating conditions for various starting materials. Subsequently, we determined the following conditions of sample preparation.

A commercial high-purity rutile (>99.9%) powder (specific surface area: 6–7 $m^2\,g^{-1}$, 0.5 g, HT0514; Toho Titanium Co., Ltd., Tokyo, Japan) was pressed uniaxially (50 MPa) into a pellet (10 mm $\phi$). The green body was sintered at 1100 °C for 2 h in air. The sample density was evaluated using Archimedes method. The surface of obtained samples was polished using diamond slurry. Then it was finished to a mirror-like surface using colloidal silica (50 nm). After polishing, the surface was annealed at 1000 °C for 1 h in air to remove stress in the surface by polishing.

The respective morphological features of the starting powder and the microstructures of obtained sintered bodies were observed using a field-emission scanning electron microscope (FE-SEM, S-800; Hitachi Ltd., Tokyo, Japan). The crystalline phase and strain in the samples were evaluated using X-ray diffraction (XRD: D8 Discover; Bruker AXS, Madison, WI, U.S.A.) with Cu Kα radiation and Raman spectroscopy (wavelength of incident beam 512 nm, Ramanor T64000; Horiba, Ltd., Kyoto, Japan). The surface roughness was evaluated using tapping-mode AFM (JSPM-5200; JEOL, Tokyo, Japan) with a Si cantilever (OMCL-AC160TS-C2; Olympus Co., Tokyo, Japan).

Wettability conversion of the sample by UV illumination was examined in ambient air using a contact angle meter (CA-X; Kyowa Interface Science Co., Ltd., Saitama, Japan) and a water droplet (1.0 μL). A Hg–Xe lamp (LA-310UV; Hayashi Watch Works, Tokyo, Japan) was used as the UV illumination source. The UV intensity was 10 mW $cm^{-2}$.

### 2.2. Evaluation of friction force variation under various conditions

In this study, the surface friction force of the samples was evaluated using FFM in contact mode with the same AFM with a Si cantilever (CSC37/AlBS; MikroMasch, Tallinn, Estonia). The nominal spring constant was 0.3 N $m^{-1}$. The measurement area was 10 μm × 10 μm. A BK7 glass cover was used to control the sample chamber atmosphere (volume of ca. 1.4 L). Under ambient air conditions (35% relative humidity, ca. $1 \times 10^4$ ppm $H_2O$ content), UV with an intensity of 10 mW $cm^{-2}$ was illuminated on the sample without putting the glass cover. The separation distance between the sample and cantilever during UV illumination was set as 50 μm. A Hg–Xe lamp with an optical-fiber coupler was used for UV illumination, but it was terminated at a set time. Then, FFM images were recorded. The scanning time necessary for each measurement area was approximately 450 s. Alternatively, under dry gas conditions, dry air ($H_2O$ content of ca. 0.5 ppm; Taiyo Nippon Sanso Corp., Tokyo, Japan) or dry nitrogen ($H_2O$ content of ca. 7 ppm; Toho Sanso Co., Ltd., Kanagawa, Japan) flowed into the sample chamber for 40 min (flow rate 2 L $min^{-1}$) after evacuating the chamber for 60 min using an oil-free diaphragm pump (pressure 1 kPa). Then, the FFM image was recorded with flowing dry gas (flow rate 0.5 L $min^{-1}$) during 10 mW $cm^{-2}$ UV illumination in the same way as that used for ambient air. Moreover, humidity control of the flowing air was conducted. After the FFM measurement conducted in dry air, wet air with relative humidity of 50% flowed into the sample chamber for 10 min (flow rate: 0.5 L $min^{-1}$) without UV illumination. Then, UV illumination was started again under the wet air condition.

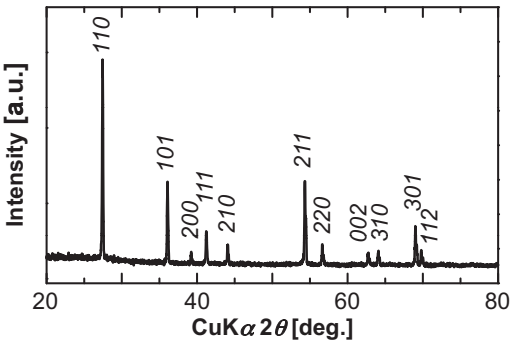


**Fig. 1.** X-ray diffraction pattern of prepared rutile ceramics.

In this study, we evaluated the friction force variation for about 70 grains under UV illumination in ambient air. Electron backscattering diffraction (EBSD) was conducted for all grains using SEM and its EBSD attachment [19] to evaluate the crystal orientation. The water contact angles of the sample before and after the FFM measurement were also measured in ambient air.

### 2.3. Evaluation of attraction and repulsion interactions by force curve measurement

Since the photoinduced hydrophilicizing rate depends on the crystal orientation [20], we employed rutile single crystal with a (1 0 0) face to evaluate attraction and repulsion interactions under UV illumination because this face provides a high photoinduced hydrophilicizing rate. A polished rutile single crystal with a (1 0 0) face (1 cm (height) × 1 cm (width) × 0.5 mm (thickness); Nakazumi Crystal Laboratory Co., Osaka, Japan) was set into the AFM. Then UV with intensity of 10 mW $cm^{-2}$ was illuminated on the sample surface. Force curve measurements were conducted using AFM with a $Si_3N_4$ coated Si cantilever (CSC38/$Si_3N_4$/AlBS; MikroMasch, Tallinn, Estonia). The approach speed was kept constant at less than 20 nm $s^{-1}$; the total piezo displacement was about 300 nm. This measurement was conducted after 0, 90, and 300 min UV illumination. During measurement, UV illumination was stopped. The separation distance between the sample and cantilever during UV illumination was set as 50 μm. The obtained deflection signal vs. the *z*-piezo position was converted into force vs. probe-to-surface separation using procedures described for our previous study [21].

## 3. Results and discussion

XRD measurements revealed that the sample is composed solely of rutile with random crystallite orientation (Fig. 1). Fig. 2 shows SEM micrographs of the starting powder and the surface of the obtained rutile ceramics. The sample grain size was nearly the expected order, and the relative density was revealed to be more than 98%. Fig. 3 shows the change of lattice parameters obtained from XRD measurement for samples as-sintered, after polishing, and after annealing at 1000 °C. This result suggests then that the

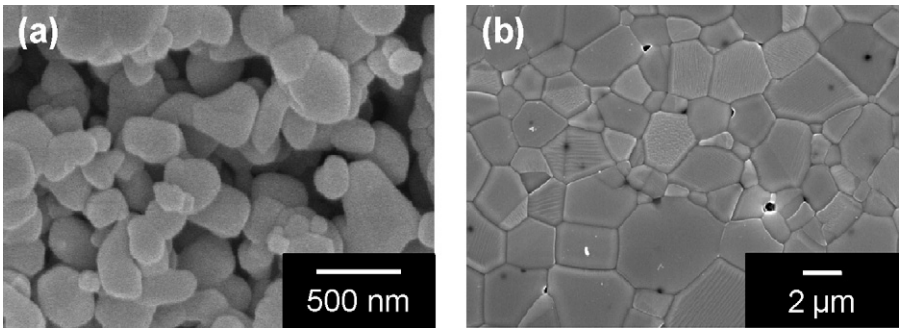


**Fig. 2.** SEM micrographs of (a) starting powder and (b) rutile ceramics surface.

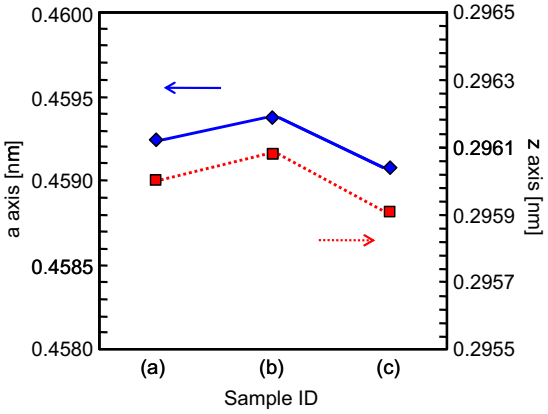


**Fig. 3.** Change of lattice parameters obtained from XRD measurement for samples as-sintered, after-polishing, and after annealing at 1000 °C.

effect of residual stress introduced to the sample surface by polishing was quite small: almost negligible. A similar result was obtained also from Raman spectra. The average roughness ($R_a$) of the rutile ceramics was about 6 nm.

Fig. 4 presents an example of the photoinduced friction force variation on the sample surface under UV illumination. The degree of friction force change depends on the grain. In this study, the friction force change under UV illumination was evaluated from four different surface positions as around 70 grains. The images of the measurement positions and stereo projection figure of corresponding grains obtained by EBSD are presented in Fig. 5. Distribution ensures the absence of bias on the crystalline orientation for the evaluated grains. Fig. 6 presents the contact angle change and corresponding average friction force variation on the sample surface under UV illumination in ambient air. During this measurement, the surface roughness variation, which is simultaneously obtainable by friction force measurement, was almost negligible. Three different stages are observable from this figure. The friction force initially increased concomitantly with increasing UV illumination time, but after a short period (around 20 min) of UV illumination, the friction force began to decrease. During this period, the contact angle decreases continuously. The friction force increases again at around 45 min UV illumination. Subsequently, it gradually increases concomitantly with increasing UV illumination. It is particularly interesting that this switching time (around 45 min) roughly corresponded to that when the water contact angle decreased and reached its saturated value. These results suggest that the photoinduced friction force variation is related to the photoinduced hydrophilicity. Because it is difficult to rationalize all these changes as caused by one mechanism, we divide them into following three stages by the friction force variation, (I) initial increase stage (0–20 min), (II) decrease stage (20–45 min), and (III) gradual increase stage (after 45 min). Then we discuss each.

The surface reaction expected in the early stage of UV illumination is photocatalytic decomposition of adsorbed organic compounds on the sample surface. As a result of decomposition of organic compounds, an increase of surface energy is expected. Assuming that the increase of surface energy ($\Delta\gamma_{SV}$) is proportional to the increase of friction force ($\Delta F$), the surface energy of grain $n$ after $t$ minutes of UV illumination is described as

$$\gamma_{SV}^{t,n} = \frac{F^{t,n}}{F^{0,n}}\gamma_{SV}^{0,n}, \tag{1}$$

where $F^{t,n}/F^{0,n}$ is the friction force ratio between $t$ and that before UV illumination, and $\gamma_{SV}^{0,n}$ signifies the initial surface energy of grain $n$ before UV illumination. Based on the Young–Dupre equation and Girifalco–Good equation [22], the relation between the contact angle and the solid surface energy is described as

$$\cos\theta \frac{2\phi}{\sqrt{\gamma_{LV}}}\sqrt{\gamma_{SV}} - 1, \tag{2}$$

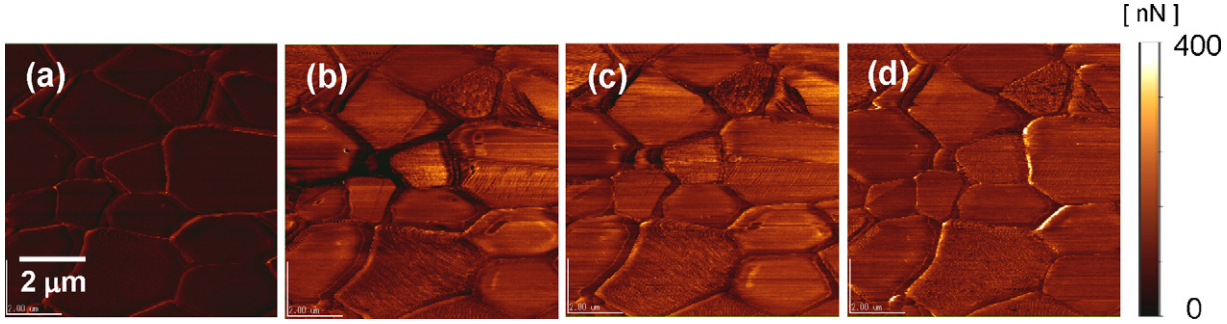


**Fig. 4.** Example of the photoinduced friction force variation on the sample surface under UV illumination (10 mW cm$^{-2}$): (a) before UV illumination, (b) after 10 min, (c) after 20 min, and (d) after 30 min.

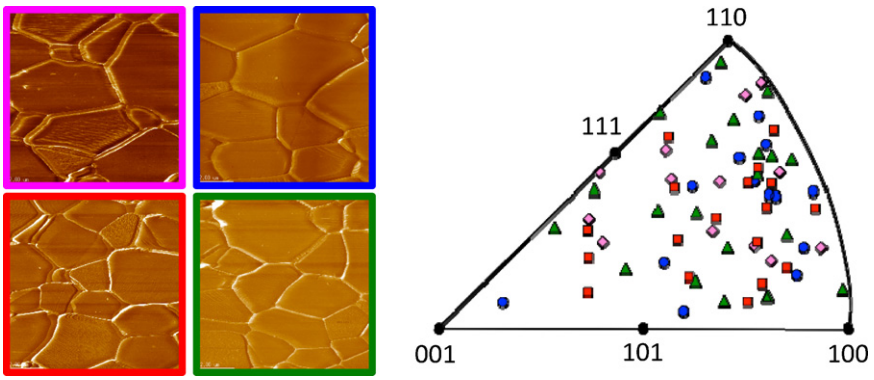


**Fig. 5.** Images of the measurement positions and stereo projection figure of corresponding grains obtained by EBSD.

where $\gamma_{LV}$ is the surface energy of liquid. Therefore, the increase of $\cos\theta$ ($\Delta\cos\theta$) for grain $n$ after $t$ minutes of UV illumination is

$$\frac{\cos\ \theta^{t,n}}{\cos\ \theta^{0,n}} = \frac{k\sqrt{\gamma_{SV}^{t,n}} - 1}{k\sqrt{\gamma_{SV}^{0,n}} - 1} = \sqrt{\frac{F^{t,n}}{F^{0,n}}} + \frac{\sqrt{(F^{t,n}/F^{0,n})} - 1}{k\sqrt{\gamma_{SV}^{0,n}} - 1} = Z\left(\frac{F^{t,n}}{F^{0,n}}\right), \quad (3)$$

where $2\phi/\sqrt{\gamma_{LV}}$ was described as a constant $k$ because $\phi$ is commonly assumed as unity. The average contact angle of the entire solid surface can be described using area ratio ($f_n$) and the contact angle of the grain ($\theta_{t,n}$), according to the Cassie–Baxter equation [23].

$$\cos\ \theta_{0,\text{avg.}} = f_1 \cos\theta_{0,1} + f_2 \cos\theta_{0,2} + \cdots + f_n \cos\theta_{0,n} \quad (4)$$

$$f_1 + f_2 + f_3 + f_4 \cdots + f_n = 1 \quad (5)$$

Substitution of Eq. (3) to Eq. (4) provides the contact angle of entire solid surface at each UV illumination period as follows.

$$\cos\ \theta_{t,\text{avg.}} = f_1 Z\left(\frac{F^{t,1}}{F^{0,1}}\right)\cos\ \theta_{0,1} + f_2 Z\left(\frac{F^{t,2}}{F^{0,2}}\right)\cos\ \theta_{0,2} + \cdots + f_n Z\left(\frac{F^{t,n}}{F^{0,n}}\right)\cos\ \theta_{0,n} \quad (6)$$

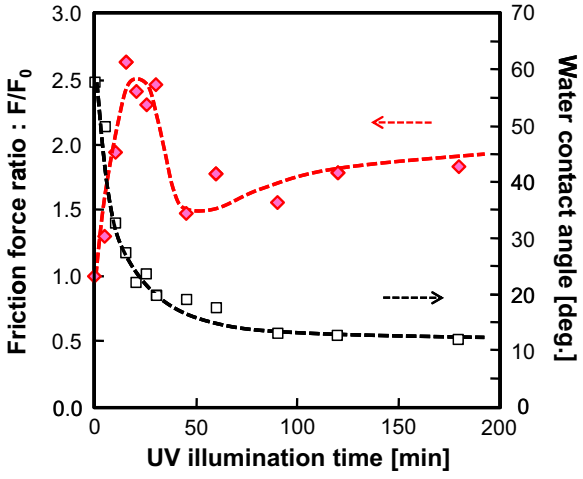


**Fig. 6.** Contact angle change and corresponding average friction force variation on the sample surface under UV illumination.

The initial contact angle of each grain ($\cos\theta_{0,n}$) was calculated by assuming that the surface energy ratio is equal to the friction force ratio between the entire surface and each grain, as shown below.

$$\gamma_{SV}^{0,n} = \frac{F^{0,n}}{F_{\text{avg.}}^{0}}\gamma_{\text{SVavg.}}^{0}, \quad (7)$$

Fig. 7 presents experimental values and calculated $\cos\theta$ for each UV illumination time. The surface energies of water (72.75 mJ m$^{-2}$ [24]) and rutile (1420 mJ m$^{-2}$ [24]) were used for this calculation. A similar trend between those of experimentally obtained results and fitted ones suggests that stage (I) is explained mainly by the photocatalytic decomposition of organic compounds and the resultant increase of friction force between the sample and cantilever. Moreover, this result suggests that the grain boundary does not serve a special role such as capillary region for water in the early stage of UV illumination.

Fig. 8 presents results of friction force measurement under dry $N_2$ and dry air. The photocatalytic reaction does not advance in $N_2$ because of the impossibility of electron transfer from $TiO_2$ [25]. Contact angles before this measurement were 58° for both. However, after 3-h measurement, it was 62° for dry $N_2$ and 20° for dry air. Therefore, no friction force increase was observed under dry $N_2$ conditions. Under dry air conditions, the friction force increased markedly after UV illumination for 50 min. The photogenerated electron transfer from $TiO_2$ to oxygen is feasible considering

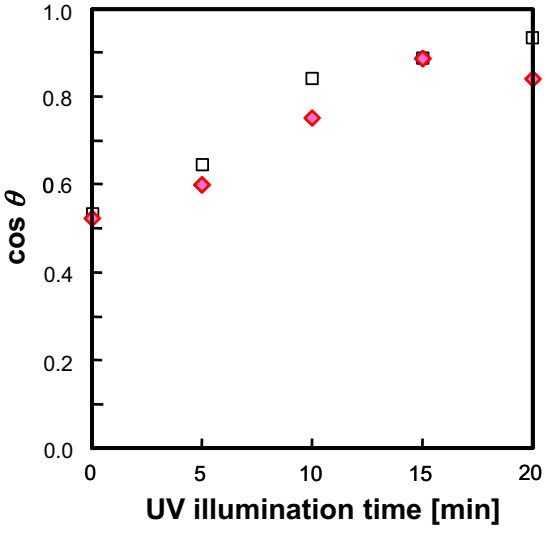


**Fig. 7.** Experimental values (black diamond) and calculated (pink square) $\cos\theta$ for each UV illumination time. (For interpretation of the references to color in this figure legend, the reader is referred to the web version of this article.)

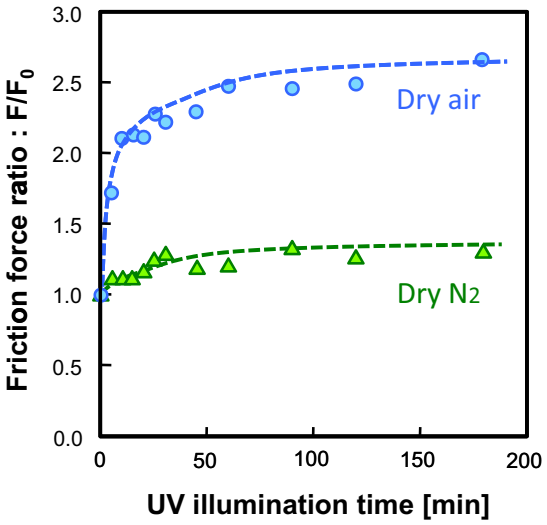


**Fig. 8.** Results of friction force measurement under dry $N_2$ and dry air.

coexisting water molecules [25]. Even dry air includes a small amount (probably less than $10^{-2}$ ppm order) of water molecules, and photocatalytic decomposition advances. It is noteworthy that the friction force in dry air increases and does not decrease, but saturates instead. This result implies that stages (II) and (III) are specific to ambient air.

Fig. 9 portrays the average friction force variation by changing humidity and UV illumination. These data represent the average of 13 grains. When UV illumination was conducted in dry air (0–180 min), the friction force was increased and saturated. Once wet air at relative humidity of 50% flowed without UV illumination (gray area), the friction force decreased rapidly. When UV was illuminated in the wet air, it began to increase. These results demonstrate clearly that the friction force variations in stages (II) and (III) are dependent on the humidity.

Based on these results, it is presumed that the decreased friction force in stage (II) is attributable to the increased hydrophilic region by water molecules on the surface, and on the resultant lubrication effect [26–30]. However, gradually increased friction force by UV illumination is observed in the highly hydrophilic stage. This change is attributed to either water condensation or the increase of water layer thickness, or both. The effect of water condensation at the tip-sample contact, with its resulting capillary effect of the water layer has been pointed out in several investigations [29,31–33]. Meanwhile, it is inferred that the excess increase of the surface water layer thickness engenders increased moving resistance of the cantilever. Recently Goertz et al. reported that the water film formed on a highly hydrophilic solid surface such as silica possesses $10^6$ times higher viscosity than bulk water [34]. Under such a condition, the moving resistance of cantilever must be increased even if the increase of the water film thickness is small. The wettability conversion in the early stage of UV illumination results from photocatalytic decomposition. However, a highly hydrophilic state might be provided by the photoinduced surface structure change of $TiO_2$.

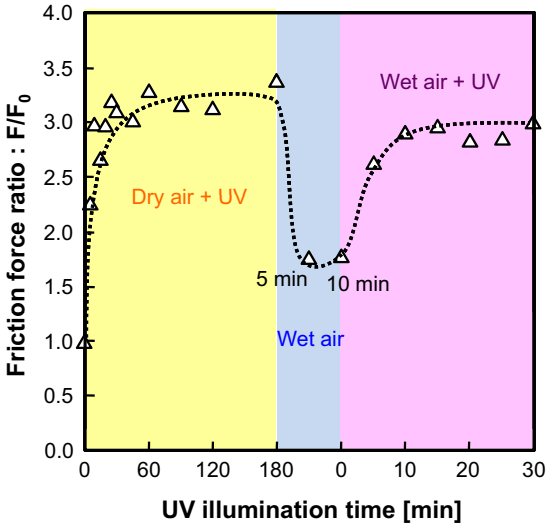


**Fig. 9.** Average friction force variation by changing humidity and UV illumination.

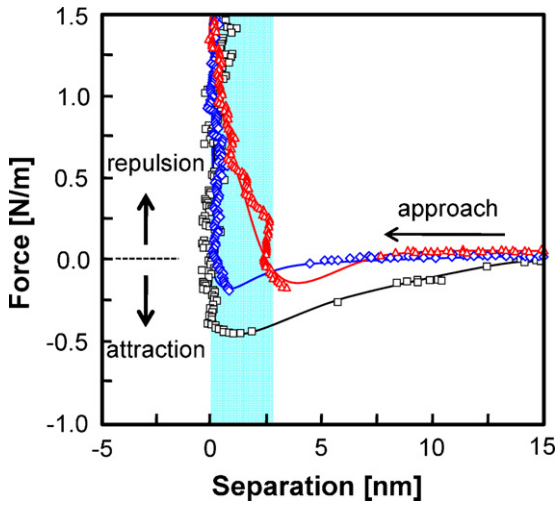


**Fig. 10.** Force curve variation on rutile single crystal (1 0 0) under 10 mW cm$^{-2}$ UV illumination: black square, before UV illumination; blue diamond, after 90 min; and red triangle, after 300 min. (For interpretation of the references to color in this figure legend, the reader is referred to the web version of this article.)

Fig. 10 shows force curve variation on rutile single crystal (1 0 0) under 10 mW cm$^{-2}$ UV illumination. This plot was obtained using a constant time interval. Therefore, the plot distance is not constant. Large distance implies rapid motion of the cantilever. Solid lines in the figure show a trajectory of the plots. Before UV illumination, attractive force works from 10 to 15 nm separation of the cantilever from the sample surface. It is deduced that organic contaminants adsorbed onto the solid surface engender the cohesive force. When UV illumination was conducted for 90 min, this attractive force had almost disappeared. After 300 min, the UV illumination, repulsive force appeared between the sample and cantilever from 2 to 3 nm separation distance. This length is almost identical to the water film thickness of hydrophilic silica reported by Goertz et al. [34], which might imply water film formation. The cantilever surface will be cleaned by the diffused active species generated from $TiO_2$ because it was set only 50 μm separation distance from the sample surface during UV illumination.

Although temperature changes before and after FFM measurements were not evaluated in this study, we believe that they were quite small: certainly less than 10 °C. The sample was not warm, even after 300 min UV illumination. We make this inference because the sample stage of the probe microscope is metal, and the heat capacity of the facility is large.

It is noteworthy that a difference exists in the trend of photoinduced friction force variation against photoinduced hydrophilicity between anatase thin films prepared from plasma crystallization process [16] and rutile ceramics. For anatase thin films, photoinduced friction force variation for UV illumination time was divisible into two stages. The decreasing stage was attributable to the pho-

tocatalytic decomposition of organic compound adsorbed onto the surface, although the increasing stage was attributed to the capillary effect or an increase in the adsorbed water layer. In the case of rutile ceramics, stage (I) appears and friction force variation for UV illumination time was divisible into three stages. A plausible explanation is the differences in photocatalytic activity, kinetics of water adsorption, and adsorption capability of water molecules on the surface. Under ambient air conditions, both water and organic contaminants such as hydrocarbons were present in the atmosphere and on the film surface. The UV intensity necessary for photoinduced hydrophilicity of anatase thin films (0.5 mW $cm^{-2}$) is much smaller than that found in this study. This result implies that the photocatalytic activity of anatase thin film is greater than rutile ceramics. It is deduced that decomposition of organic compounds and water adsorption advances rapidly on anatase thin film. In the case of rutile, the kinetics of these two phenomena are slow and adsorption capability of water is not large. Therefore, stage (I) is not observed in anatase. Moreover, very recently, it was revealed that a thin (ca. 10 nm) porous amorphous $TiO_2$ layer is formed on the surface of anatase films prepared from plasma crystallization process [35]. Differences in surface roughness and residual stress might also contribute to the difference. A detailed investigation of the origin of difference in friction force variation between these two crystalline phases will be undertaken in future work.

## 4. Conclusion

The photoinduced friction force variation for the surface of rutile polycrystalline ceramics was investigated. The photoinduced friction force variation is divisible into three stages: an initial increase stage, decrease stage, and gradual increase stage. The initial increase stage is attributed to the photocatalytic decomposition, whereas the decrease stage and gradual increase stage are attributed to the lubrication effect and either a capillary effect or the increased adsorbed water layer. From force curve measurements on the highly hydrophilic rutile single crystal (1 0 0), the repulsion force was measured from a 2 to 3 nm separation distance.

## References

[1] A. Fujishima, K. Honda, Nature 37 (1972) 238–245.
[2] T. Kawai, T. Sakata, Nature 286 (1980) 474–476.
[3] D.F. Ollis, H. Al-Ekabi (Eds.), Photocatalytic Purification and Treatment of Water and Air, Elsevier, Amsterdam, London, New York, Tokyo, 1993, p. 747.
[4] I. Rosenberg, J.R. Brock, A. Heller, J. Phys. Chem. 96 (1992) 3423–3428.
[5] N. Takeda, T. Torimoto, S. Sampath, S. Kuwabata, H. Yoneyama, J. Phys. Chem. 99 (1995) 9986–9991.
[6] M.R. Hoffmann, S.T. Martin, W. Choi, D.W. Bahnemann, Chem. Rev. 95 (1995) 69–96.
[7] R. Wang, K. Hashimoto, A. Fujishima, M. Chikuni, E. Kojima, A. Kitamura, T. Shimohigoshi, T. Watanabe, Nature 388 (1997) 431–432.
[8] A. Fujishima, K. Hashimoto, T. Watanabe, $TiO_2$ Photocatalysis: Fundamentals and Applications, BKC Inc., Tokyo, 1999, p. 66.
[9] T. Zubkov, D. Stahl, T.L. Thompson, D. Panayotov, O. Diwald, J.T. Yates, J. Phys. Chem. B 109 (2005) 15454–15462.
[10] C.Y. Wang, H. Groenzin, M.J. Shultz, Langmuir 19 (2003) 7330–7334.
[11] N. Sakai, A. Fujishima, T. Watanabe, K. Hashimoto, J. Phys. Chem. B 107 (2003) 1028–1035.
[12] M. Miyauchi, A. Nakajima, A. Fujishima, K. Hashimoto, T. Watanabe, Chem. Mater. 12 (2000) 3–5.
[13] R. Wang, K. Hashimoto, A. Fujishima, M. Chikuni, E. Kojima, M. Shimohigoshi, T. Watanabe, Adv. Mater. 10 (1998) 135–138.
[14] K. Katsumata, A. Nakajima, H. Yoshikawa, T. Shiota, N. Yoshida, T. Watanabe, Y. Kameshima, K. Okada, Surf. Sci. 579 (2005) 123–130.
[15] A. Nakajima, S. Koizumi, T. Watanabe, K. Hashimoto, Langmuir 16 (2000) 7048–7050.
[16] N. Arimitsu, A. Nakajima, T. Watanabe, Y. Kameshima, K. Okada, J. Photochem. Photobiol. A: Chem. 203 (2009) 155–160.
[17] A. Miyamura, K. Kaneda, Y. Sato, Y. Shigesato, Thin Solid Films 516 (2008) 4603–4608.
[18] T. Shibata, H. Irie, K. Hashimoto, J. Phys. Chem. 107 (2003) 10696–10698.
[19] J. Kameda, A. Yamagishi, T. Kogure, Am. Mineral. 90 (2005) 1462–1465.
[20] R. Wang, N. Sakai, A. Fujishima, T. Watanabe, K. Hashimoto, J. Phys. Chem. B 103 (1999) 2188–2194;
A. Nakajima, A. Nakada, N. Arimitsu, Y. Kameshima, K. Okada, Mater. Lett. 62 (2008) 1319–1321.
[21] T. Isobe, Y. Nakano, Y. Kameshima, A. Nakajima, K. Okada, Appl. Surf. Sci. 255 (2009) 8710–8713.
[22] M. Imoto (Ed.), Hyoumenchouryoku no rikai no tameni, Koubunnshi kannkoukai, Tokyo, 1993, p. 74 (in Japanese).
[23] A.B.D. Cassie, S. Baxter, Trans. Faraday Soc. 40 (1944) 546–551.
[24] A. Nakajima (Ed.), Kotaihyoumen no nureseigyo, Uchida rokaku-ho Press, Tokyo, 2007, p. p. 45 [in Japanese].
[25] Y. Nosaka, A. Nosaka (Eds.), Nyumon Hikari Shokubai, Tosho Press, Tokyo, 2004, pp. 63–87 (in Japanese).
[26] L. Xu, H. Bluhm, M. Salmeron, Surf. Sci. 407 (1998) 251–255.
[27] J. Hu, X.D. Xiao, D.F. Ogletree, M. Salmeron, Surf. Sci. 327 (1995) 358–370.
[28] A.A. Feiler, P. Jenkins, M.W. Rutland, J. Adhes. Sci. Technol. 19 (2005) 165–179.
[29] W. Karino, H. Shinbo, Tribol. Int. 40 (2007) 1568–1573.
[30] R.R.M. Zamora, C.M. Sanchez, F.L. Freire Jr., R. Prioli, Phys. Status Solidi A 201 (2004) 850–856.
[31] L. Sirghi, T. Aoki, Y. Hatanaka, Thin Solid Films 422 (2002) 55–61.
[32] L. Sirghi, T. Aoki, Y. Hatanaka, Surf. Rev. Lett. 10 (2003) 345–349.
[33] A. Opitz, S.I.U. Ahmed, J.A. Schaefer, M. Scherge, Surf. Sci. 504 (2002) 199–207.
[34] M.P. Goertz, J.E. Houston, X.-Y. Zhu, Langmuir 23 (2007) 5491–5497.
[35] T. Watanabe, Y. Yokota, N. Yoshida, Y. Shibayama, H. Ohsaki, Ceram. Trans. (2010) 149–160.